Change Detection with GRASS GIS – Comparison of images taken by different sensors

Michael Fuchs, Rainer Hoffmann and Friedhelm Schwonke
Federal Institute for Geosciences and Natural Resources (BGR)
`michael.fuchs@bgr.de`

Keywords: Remote Sensing, Change Detection, diversity, GRASS, Yemen

Abstract

Images of American military reconnaissance satellites of the Sixties (CORONA) in combination with modern sensors (SPOT, QuickBird) were used for detection of changes in land use. The pilot area was located about 40 km northwest of Yemen's capital Sana'a and covered approximately 100 km². To produce comparable layers from images of distinctly different sources, the moving window technique was applied, using the diversity parameter. The resulting difference layers reveal plausible and interpretable change patterns, particularly in areas where urban sprawl occurs.

The comparison of CORONA images with images taken by modern sensors proved to be an additional tool to visualize and quantify major changes in land use. The results should serve as additional basic data eg. in regional planning.

The computation sequence was executed in GRASS GIS.

Introduction

GRASS GIS (http://grass.osgeo.org) with extended functionality and operability is more than a common geographic information system. It is powerful in raster data processing, offers fundamental functions in terrain- and landscape analysis with extended tools for hydrological modeling and a small functionality for remote sensing. Furthermore it can be used to process three dimensional data. This powerful functionality can be used as a frame for studies, which use GIS in combination with remote sensing tools.

Change Detection – State of the art

Change Detection is a group of methods commonly used in remote sensing. Because of the repetitive coverage of earth orbiting satellites at short intervals and consistent image

quality, methods of Change Detection have become part of environmental observation systems (Lunetta & Elvidge 1999; Owe 2007).

Change Detection is defined as: "The sensing of environmental changes that uses two or more scenes covering the same geographic area acquired over a period of time." (Glossary of Canada Centre for Remote Sensing, http://www.ccrs.nrcan.gc.ca/glossary) Aside from visual interpretation different algorithms are applied.

Essential aims of Change Detection are:

- Detection and evaluation of land use changes

- Support the monitoring of disasters triggered by geological, meteorological or man made factors.

The use of Change Detection algorithms requires two preconditions:

1. Changes in land cover must result in changes in radiance values.

2. Changes in radiance due to land cover changes must be large with respect to radiance changes caused by other factors, such as atmospheric conditions, sun angle or vegetation phenology.

The preconditions mentioned are based on processing scenes from the same sensor type. The scenes acquisition should be done carefully because differences in radiation, precipitation and surface temperature in combination with phenological variations lead to discrepancies in reflectance properties. These sources of interference have to be extensively eliminated. The phenological variations are reduced by using scenes taken at the same season of the year. Additionally, climate data should be available to assess the phenological stage of the vegetation.

Well-known satellite missions have been operating continuously for decades. Landsat missions for instance have been delivering images since 1972 with repetition rates of 18 days (MSS) and 16 days (Landsat 4, 5, 7), respectively.

The data preparation includes:

- Image registration with geometric correction

- Radiometric calibration with atmospheric correction

The goal is to achieve high quality images with geographic precision of less than one pixel and correlation of radiometric calibration close to 1.

The applied methods of Change Detection comprise simple difference procedures and multivariate statistical routines. Change Detection can be used directly to multiband stacks or derived resp. classified layers. An overview of Change Detection methods can be found in Théau (2006), the comparison and evaluation of methods and their applicability is described in Peinado (2001). Some major definitions used in remote sensing are given below according to Théau (2006) and Yang (1999):

- Image differencing

- NDVI, Tasseled Cap

	MODIS	**Landsat**	**SPOT**	**QuickBird**
Continuity	Since 1999	Since 1972	Since 1986	Since 2002
Spatial Coverage	2330 km (cross track) by 10 km (along track at nadir)	170 x 183 km	60 x 60 km	16.5 x 16.5 km
Spatial Resolution	250 m (bands 1-2) 500 m (bands 3-7) 1000 m (bands 8-36)	30 m (pan 15 m)	10 m (pan 5 or 3 m)	2.44 m (pan 0.61 m)
Band Numbers	Multispectral (36) (hyper spectral)	Multispectral (7) + panchromatic	Multispectral (4) + panchromatic	Multispectral (4) + panchromatic
Repetition	2 days	16 days	2.5 – 26 days	1 – 3.5 days
Acquisition Costs	free	selective imagery free, further cost 0.02 \$/km^2	0.94 \$/km^2	22 \$/km^2

Tab.1: Technical Data of Selected Remote Sensing Satellites

The Tasseled Cap transformation (TC) optimizes data viewing for vegetation studies as one of the available methods for enhancing spectral information content of Landsat TM. Four bands are calculated: brightness, greenness, wetness, and haze.

- Image rationing

- Principal Components Analysis (PCA)

This technique is usually used to reduce the number of spectral components (spectral bands) to fewer principal components accounting for the most variance in the original multispectral images. Image spectral bands of two or more dates are treated as a single data set. After performing PCA, information that is common to multidate images is mapped to the first component (unchanged areas) whereas information that is unique to one of the dates is mapped to the following components (changed areas).

- Composite Analysis

Supervised and unsupervised classifications are used to analyze these datasets. Classes where changes occurred are expected to present statistics significantly different from where changes did not take place.

- Change Vector Analysis

- Comparison of post-classifications

The critical step of all mentioned methods is deciding where to place the threshold for changes. Furthermore the exact nature of the changes needs a careful interpretation including the knowledge of the investigation area including ground checks.

Reconnaissance Satellite Photos – CORONA

The term stands for a series of U. S. Military reconnaissance satellites (KH 1 to KH 5) which were operated between 1959 and 1972. The satellites of the CORONA series delivered panchromatic photographs of many areas of the world.

Images of the first generation were declassified at the end of the Nineties. The ground resolution of the two KH-4 systems (1963 – 1972) ranged between 2 and 3 m. The photographs are 30 $ each and can be ordered under http://edcsns17.cr.usgs.gov/EarthExplorer.

CORONA photos are used in various research projects. One application is the derivation of elevation models because many scenes provide stereoscopic records (Schmidt et al. 2001). Grosse et al. (2005) used CORONA images for the visual interpretation of thermokarst processes. Another area of application comprises the preparation and support of archeological excavations (Goossens et al. 2002). In geological mapping CORONA images are required where other high resolution images are missing. Lorenz (2004) completed the mapping of Paleozoic stratums in Russian Arctic with CORONA images.

Method

CORONA images are an essential source of information in particular for those decades where other high resolution images are missing. This applies to the sixties of the last century when only military reconnaissance satellites were operating. However, only Corona images are available for this decade since 1996 (http://edc.usgs.gov/guides/disp1.html).

The methods of Change Detection mentioned above are based on scenes taken by the same sensor type at different dates. The method described in this paper is based on the image differencing method. Scenes are compared that were taken by different sensors. For this, the steps for the preparation and harmonization of the image information are very important. These working steps comprise the geometric correction of the CORONA image, the transformation of the RGB channels of the modern satellite data into one panchromatic channel and the resample process into the pixel resolution of the CORONA image. Then the subsequent moving window algorithm can be applied. The computation sequence ends with the subtraction step (Fig. 1).

The core of the computation sequence uses the moving window technique. This technique is offered by the GRASS raster module r.neighbors (http://grass.osgeo.org). The command r.neighbors can be run with different parameters. Basically two groups of parameters exist. The first group comprises the statistical parameters. The second group comprises parameters commonly used in landscape analysis (McGarigal & Marks 1995). These two parameters are the diversity and the interspersion. Diversity is defined as the number of different values within the neighborhood. The computation with parameters of the second group leads to results which calculate pixelwise diversity as dimensionless value. Therefore the comparison between images taken with different sensors is possible as outlined now.

For each pixel the number of different neighborhood pixel values has to be identified and stored as a new value. Therefore the size of the moving window is to be considered as sensible value with strong influence on the result layers (Fig 2). The size of the moving window has
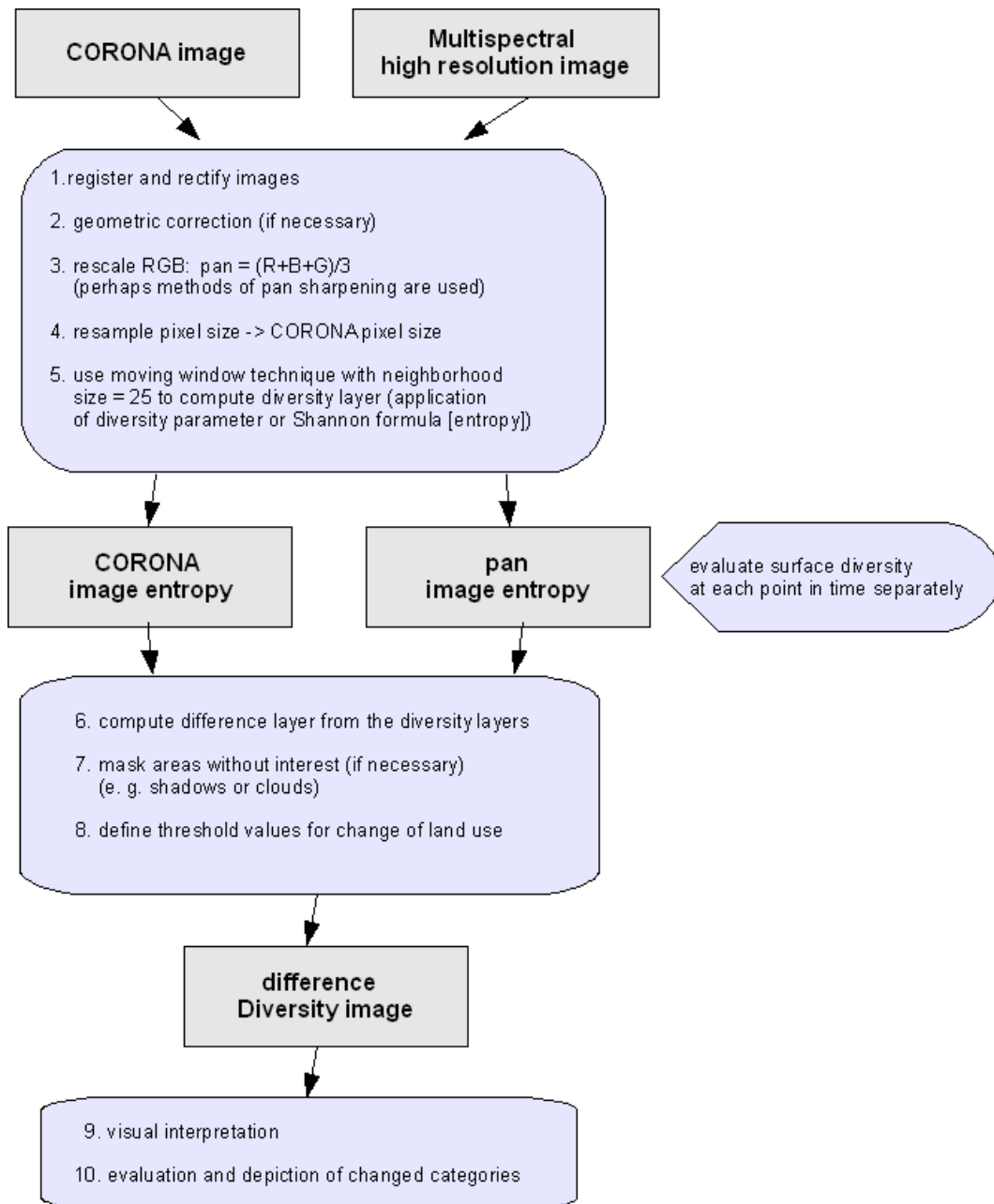
Fig. 1: Flow chart of sequential computation

strong influence on the pattern of diversity. Tests show that the matrix size of 25x25 delivers interpretable result layers; hence 625 neighboring cells are included in the computation. With the pixel size of 2.5 m, the radius of influence is 12 * 2.5 m = 30 m (leaving out the central pixel).

In addition to the diversity parameter the entropy formula (Eq. 1) is used in the computation. The Shannon Diversity Index (SHDI) is computed in our own application written in Fortran 90 and the results are dumped as absolute values. The SHDI is based on the information theory and is also called as Negentropy (Palm 1985). It presents the amount of information
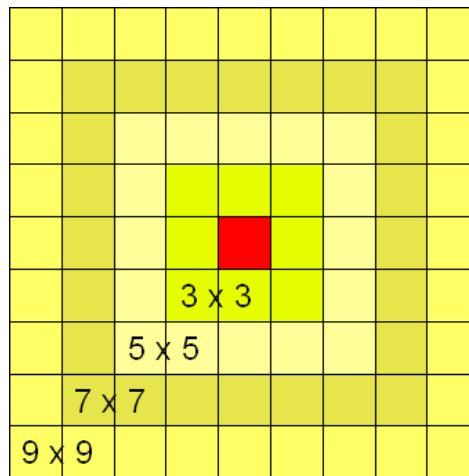
Fig 2: Inclusion of neighborhood size in the moving window

for a defined quantity. The entropy formula is commonly used in different research areas, such as landscape analysis (McGarigal & Marks 1995). In soil geography it is called areal heterogeneity. Here the entropy is a measure of uncertainty. In this discipline it was discussed as indicator of landscape structure (Altmann & Haase 1987). The measure of uncertainties for a defined quantity of information is basis of evaluations in human geography (Paulov 1991) and it is discussed in cartography to support the process of generalization (Bjorke 1996).

$$SHDI = -\sum_{i=1}^{m}(p_i * ln\, p_i) \quad (1)$$

- *with range: 0 – ln m*
- *pi – Proportion of number of one value to values total*
- *m – Count of different values*
- *SHDI=0 if window contains the same value in all cells.*
- *SHDI increases with the number of different values in the window.*
- *Maximum entropy is reached when all values are different, the same as ln m.*

The result layers are intersected by subtraction. Sources of error originating from clouds or shadows can be masked. Therefore results of supervised or unsupervised classifications can be used because such classes normally have a good delineation from other classes in the multivariate space.

Area of investigation and data input layer

The test site is located north west of Yemen's capital Sana'a and comprises an area of 10 x 10 km. In this arid to semi-arid climate zone, an ancient cultivated land with deficiencies of water occurs. The test site is composed of a cuesta landscape with altitudes between 2500 and 3000 m a.s.l. with wide-stretched valleys and a network of wadis (Fig. 3). Farming within the test site is characterized by extensive irrigation using groundwater from wells. On a limited scale run-off water is used, too. Arable land mainly is located in the valleys and on

man-made terraces located on the pediments in front of the escarpments and on dip slopes. Aside from land use such as arable farming, various other categories of land use can be found (Fig. 4).

Due to the long term technical cooperation between the geological surveys of the Republic of Yemen and Germany, there are satellite images available in the Federal Institute for Geosciences and Natural Resources (BGR). For this study SPOT data (http://www.spot.com) and GoogleEarth-QuickBird data (http://earth.google.com) were chosen for the comparison with CORONA images (Tab. 2).

Fig. 3: View to the investigation area northeast of Shibam city, Yemen (photo R. Kringel 11/2006, BGR)

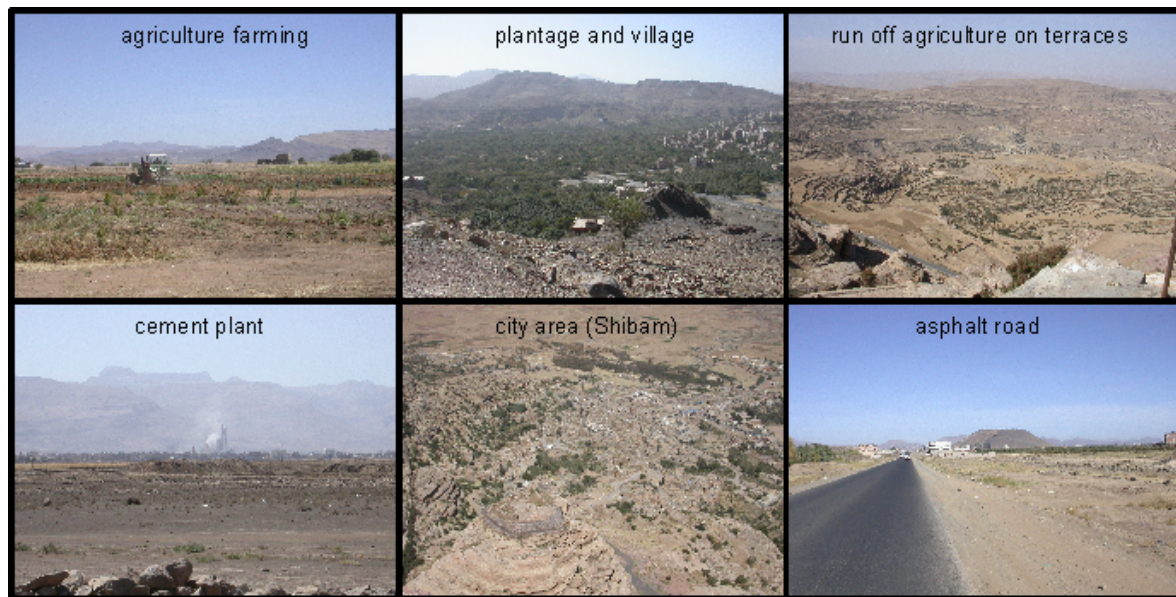| Sensor type	Spectral bands	Spatial resolution [m]	Date	Source
CORONA	panchromatic	2.5	07.11.1967	USGS (http://www.usgs.gov)
QuickBird	color composite	0.6	14.11.2003	Google Earth (http://earth.google.com)
SPOT	RGB, NIR + panchromatic	10 + 2.5	23.04.2004	SPOT IMAGE (http://www.spot.com)

Tab. 2: Images used

Fig 4: Exemplary land uses in the study area (photos by R. Kringel 11/2006, BGR)

Results

The first results contain the computed diversity layers derived from the panchromatic images. The diversity/heterogeneity is quantified at date A (Fig. 5) and date B (Fig. 6 -7). Areas with low and high diversity can be delineated and combined with land cover classes. The two entropy layers of QuickBird (Fig. 7) and SPOT (Fig. 6) data show identical patterns in heterogeneity. This is confirmed by the correlation of 0.84 (Tab. 4). In contrast the comparison of diversity between the CORONA image and the modern scenes shows no correlation (Tab. 4).

layer	minimum	maximum	mean	variance
CORONA panchromatic	0	248	152.4	2348.0
CORONA entropy	0	4.98	3.97	0.65
CORONA diversity	1	172	85.5	941.2
QuickBird panchromatic	0	254	116.6	1338.6
QuickBird entropy	0	5.25	4.16	0.29
QuickBird diversity	1	224	100.2	1287.4
SPOT panchromatic	0	230	75.3	245.9
SPOT entropy	0	4.48	3.1	0.21
SPOT diversity	1	118	34.4	166.4
CORONA-QickBird entropy difference	-5.08	3.16	-0.19	0.58
CORONA-QuickBird diversity difference	-193	130	-14.7	1280.5
CORONA-SPOT entropy difference	-4.06	2.81	0.87	0.61
CORONA-SPOT diversity difference	-84	139	51.1	852.8

Tab. 3: Univariate statistics for input and output layers

The entropy layers mark agriculture terraces, plantations, infrastructure, and settlement areas

as highly divers. The visible patterns with high entropy coincide with the border areas of Wadis. This can be explained by intensive human activities and changes in land use. Parts with low entropy comprise areas covered by clouds or shadows, areas on the higher part of the plateaus as well as barren land.
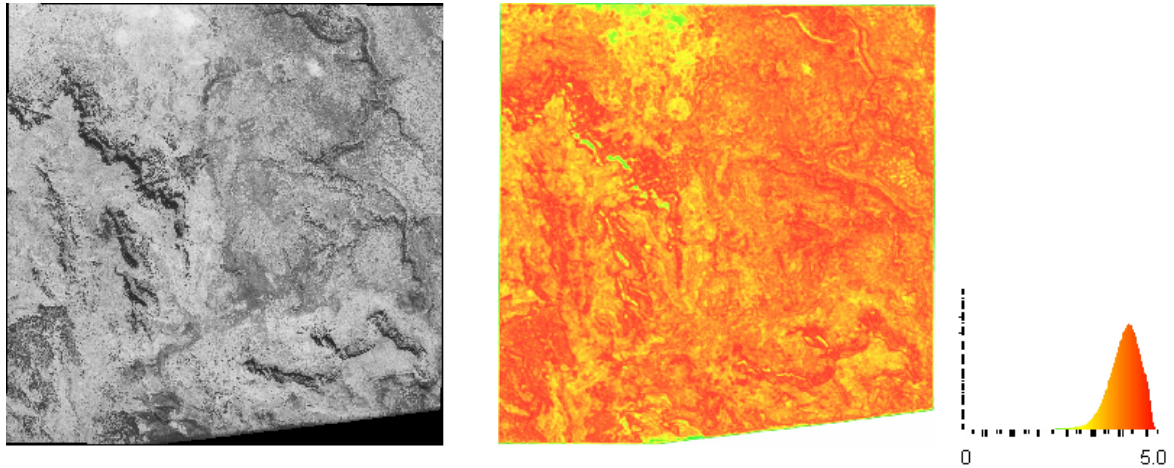

Fig. 5: CORONA image (left), its entropy pattern (middle), and distribution of entropy values (right)
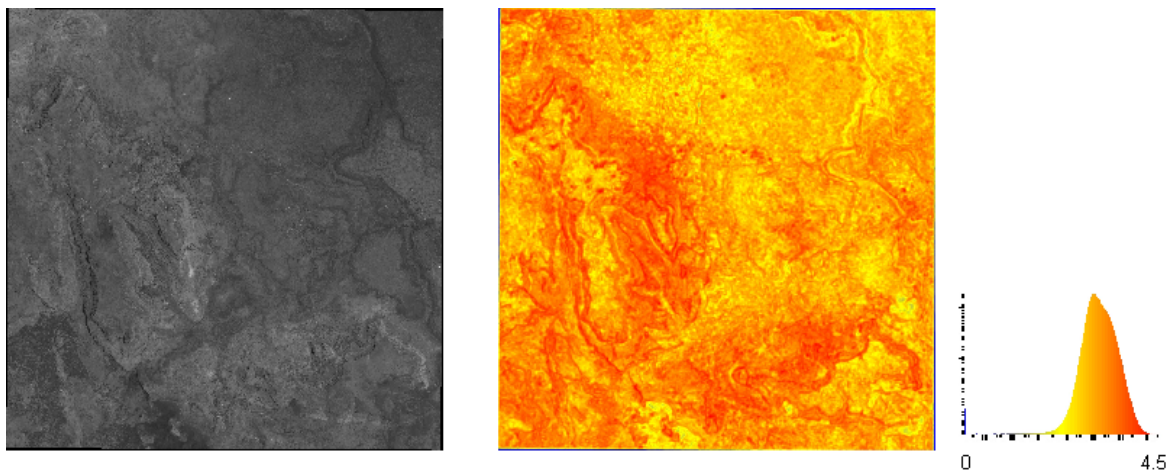

Fig. 6: SPOT panchromatic image (left), its entropy pattern (middle), and distribution of entropy values (right)

entropy layer	QuickBird	SPOT
CORONA	0.43	0.34
QuickBird		0.84

Tab. 4: Correlation coefficients between the entropy layers

The difference images (difference = CORONA entropy – panchromatic image entropy) illustrate the intensity of change between date A and date B. Areas with shadows and cloud cover have to be neglected, although high differences can occur. For these areas an assessment of change is not possible. The threshold between change and no change is drawn in the middle
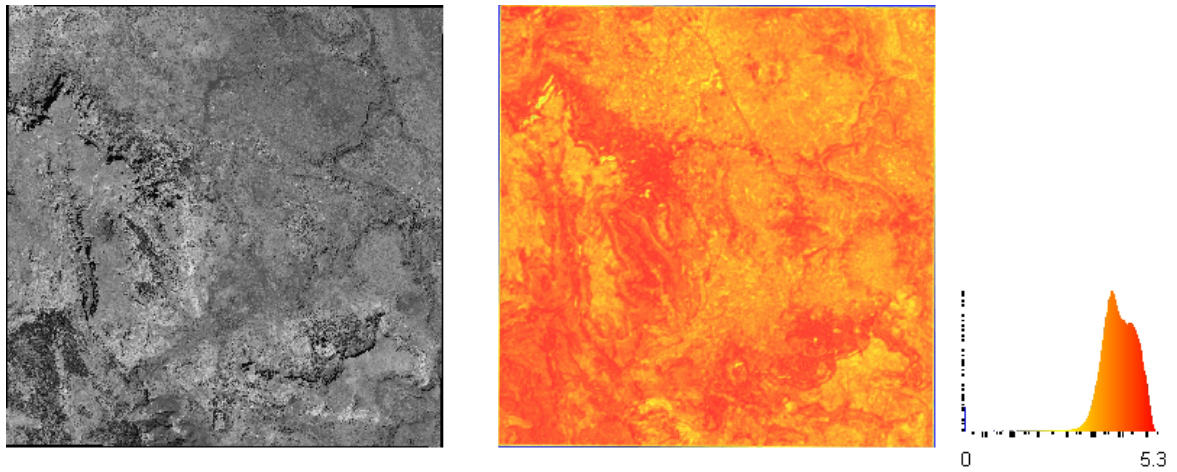
Fig. 7: QuickBird panchromatic image (left), its entropy pattern (middle), and distribution
of entropy values (right)

of the distribution of difference values. A negative value stands for change. The smaller the
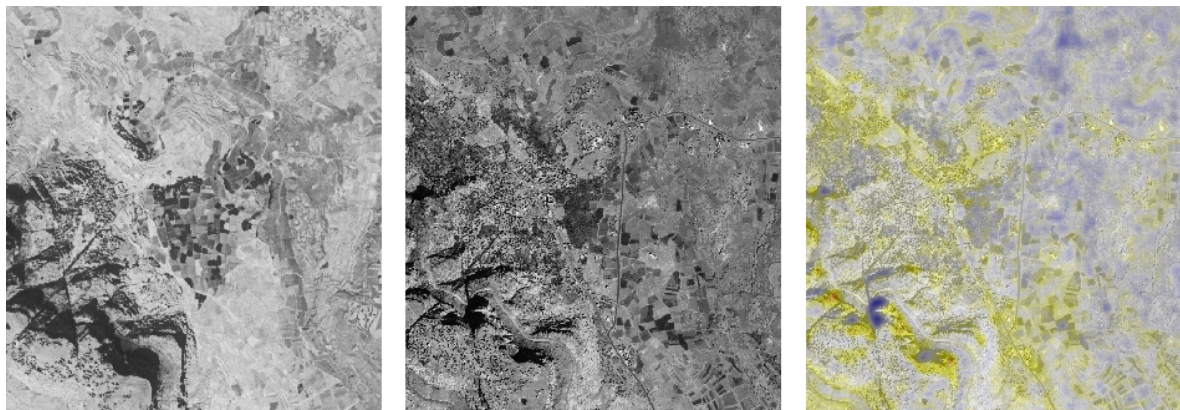values the stronger is the change (Tab. 3).

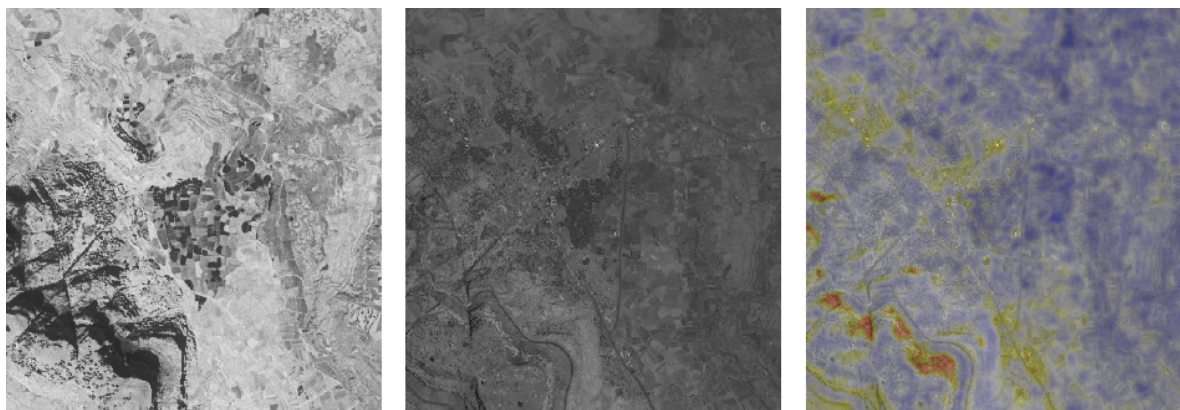Fig. 8: CORONA, QuickBird image and entropy difference layer of Shibam

Fig. 9: CORONA, SPOT image and entropy difference layer of Shibam

The city of Shibam is located in the center of the test site (Fig. 8, 9). In this 2.5 km² clipping area the readability of the entropy difference pattern is depicted (Fig. 8, 9). Negative difference values have an orange-yellow coloring and are plotted transparently on the panchromatic image. Areas with very strong differences are marked by shadows (visible along the geological fault zone, Fig 8 and 9 left). These areas were not considered in the final generalization pattern. The remaining pattern clearly reflects the distribution of building areas and infrastructure at the edge of the town as well as changes in land use. Therefore both resulting entropy difference layers show an identical pattern.

Shadows and clouds were eliminated for the difference patterns by masking and the remaining patterns were generalized. As result several categories can be distinguished (Fig. 10):

- extension of settlements (1)

- urban sprawl as result of construction of new roads (2)

- plant settlement (3)

- extension of plantation (4)

The areas shown in Fig. 10 mark the areas with changes due to human activities. Even in this rural area changes in infrastructure – mainly construction of new roads – and urban sprawl are clearly visible. During the last four decades the changes have reached a considerable dimension so that the size of the city now is twice as large.

The use of CORONA images for Change Detection (simple image differencing method) increases the evaluated period by one decade. The entropy and diversity difference images show plausible and interpretable change pattern. The comparison of CORONA images of the Sixties with images taken by modern sensors turned out to be a promising complement approach to visualize and quantify major changes in land use.

References

1. Altmann, R.; Haase, G. (1987): Zur Kennzeichnung von Merkmalsvariabilität, Kontrast und Arealheterogenität als Eigenschaften der Landschaftsstruktur". Strukturen und Prozesse in der Geographie: Beiträge zur quantitativ arbeitenden Geographie, Band 19, 145-154, Haack: Gotha.

2. Bjorke, J. (1996): Framework for Entropy-based Map Evaluation. Cartography and Geographic Information Systems, 23, 2, 78-95.

3. GRASS (2008): Geographic Resources Analysis Support System, GRASS GIS 6.3.0 http://grass.osgeo.org

4. Grosse, G.; Schirrmeister, L.; Kunitsky, V. V.; Hubberten, H.-W. (2005): The Use of CORONA Images in Remote Sensing of Periglacial Geomorphology: An Illustration from the NE Siberian Coast. Permafrost and Periglac. Process. 16: 163–172.

5. Goossens, R.; De Man J.; De Dapper M. (2001): Research on the possibilities of CORONA-satellite-data to replace conventional aerial photographs in geo-archaeological
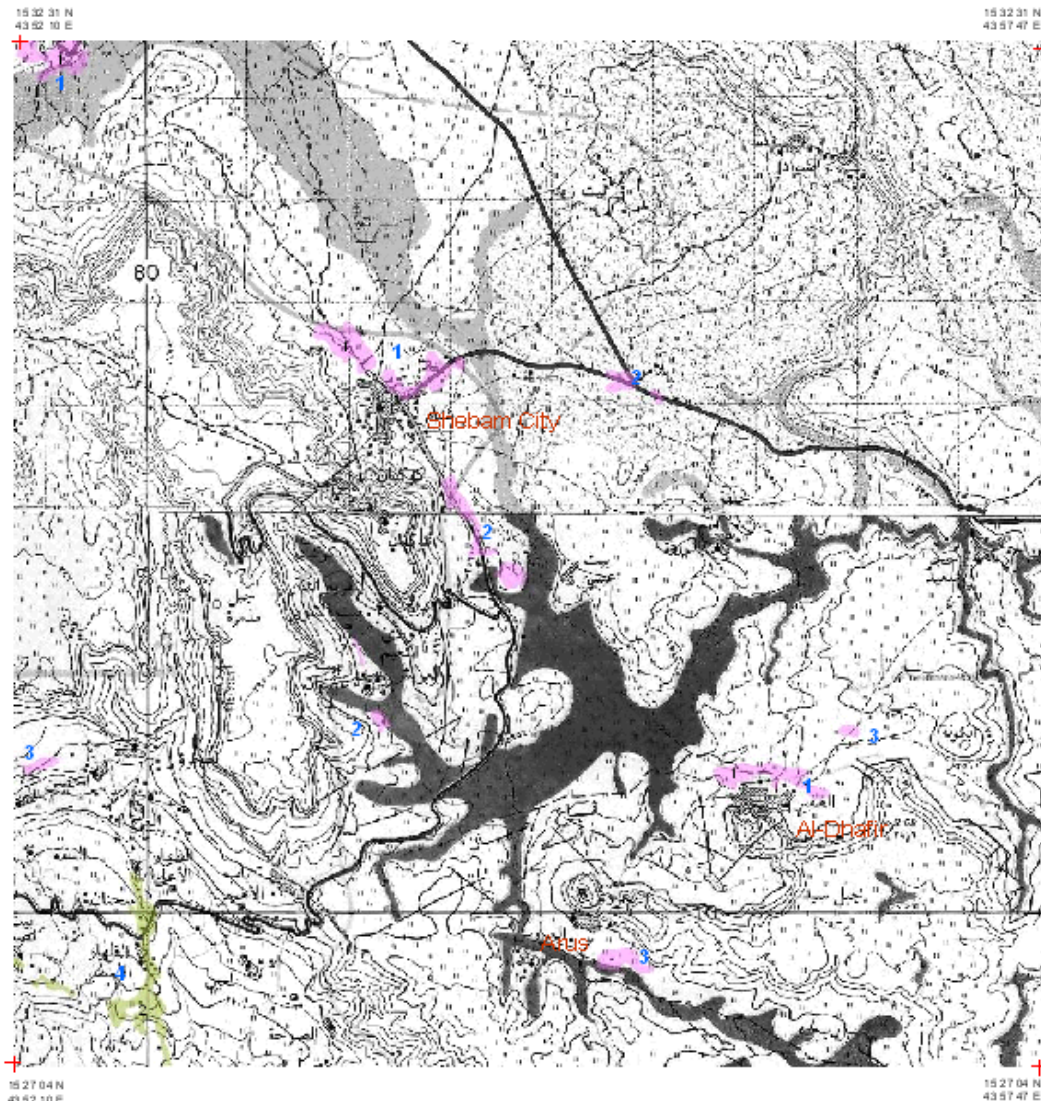
Fig. 10: Changes in land use marked on topographic map from the eighties.

studies, practised on Sai (Sudan). In A Decade of Trans-European Remote Sensing Co-operation, Buchroithner MF (ed.). Balkema Publishers: Lisse/Netherlands; 257–262.

6. Lorenz, H. (2004): Integration of Corona and Landsat Thematic Mapper data for bedrock geological studies in the high Arctic. International Journal of Remote Sensing, Volume 25, Number 22: 5143-5162.

7. Lunetta, R. S.; Elvidge, Ch. D. (eds.) (1999): Remote sensing change detection: environmental monitoring methods and applications, Taylor & Francis, London.

8. McGarigal, K.; Marks B. J. (1995): FRAGSTATS: spatial pattern analysis program for quantifying landscape structure. USDA For. Serv. Gen. Tech. Rep. PNW-351.

9. Owe, M. (ed.) (2007): Remote sensing for environmental monitoring and change detection: a compilation of papers presented at the IAHS Symposium on Remote Sensing

for Environmental Monitoring and Change Detection, in Perugia, as part of the 24th
IUGG General Assembly, 2007, IAHS publication, 316.

10. Palm, G. (1985): Information und Entropie. In: Natur und Wissenschaft. Konkursbuch
14, Zeitschrift für Vernuftskritik, 95-110. Tübingen: Konkursbuchverlag.

11. Paulov, J. (1991): Entropie in der Humangeographie – Einleitende konzeptionelle Übersicht.
Petermanns Geographische Mitteilungen 2/1991, 89 – 97, Gotha: Haack.

12. Peinado, L. O. (2001): Comparison of Change Detection Methods for the Extraction of
Land Cover Parameters. Herbert Utz.

13. Schmidt, M.; Goossens, R.; Menz, G.; Altmaier, A.; Devriendt, D. (2001): The use
of CORONA satellite images for generating a high resolution digital elevation model.
IEEE vol. 7: 3123 – 3125.

14. Théau, J. (2006): Detection of Changes Using Remote Sensing: an Overview of Princi-
ples and Applications. Geo-Spatial and Range Sciences Conference, online[1].

15. Yang, X. M. (1999): Change Detection Based on Remote Sensing Information Model and
its Application on Coastal Line of Yellow River Delta. GISdevelopment-Proceedings,
online[2].

---

[1]http://giscenter.isu.edu/gisday/grsc_archives/chdetection.pdf
[2]http://www.gisdevelopment.net/aars/acrs/1999/ps5/ps5043.asp

---